

Nuclear Internal Momentum Distributions*

JOHN M. WILCOX AND BURTON J. MOYER

Radiation Laboratory, Department of Physics, University of California, Berkeley, California

(Received February 28, 1955)

The nuclear internal momentum distributions of protons in light nuclei have been studied with the 340-Mev scattered proton beam from the synchrocyclotron. The two protons from a quasi-elastic scattering event are detected in coincidence, and the energy of one of them is magnetically analyzed. In the limit of the impulse approximation, conservation of energy and momentum can be employed to solve for the momentum of the struck proton. The best fit to the experimental data for beryllium was obtained with a Gaussian momentum density distribution with a $1/e$ value of about 20 Mev. Fermi (rectangular) and Chew-Goldberger distributions did not fit so well. Qualitative differences were

observed between lithium, beryllium, and boron. The observed lithium spectrum was interpreted as being caused by two types of protons in lithium; two core protons that have a large momentum distribution and a third proton that has a rather low kinetic energy. This speculation was supported by the shape of the observed lithium spectrum, and by the relative yields from lithium, beryllium, and deuterium. The spectrum observed from beryllium indicated that the protons in beryllium have a larger momentum than the protons in the lighter elements studied. There were some indications that the fifth proton in boron may behave similarly to the third proton in lithium.

I. INTRODUCTION

ONE of the basic properties of the atomic nucleus is the momentum distribution with which the neutrons and protons are moving inside the nucleus. If the correct nuclear spatial wave function were known, then by a fundamental quantum-mechanical principle we could obtain the momentum-density distribution as follows.

If $\psi(\mathbf{r})$ is the solution of the Schrödinger equation, then the wave function in momentum space $\phi(k)$ can be found by a Fourier transform¹

$$\phi(\mathbf{k}) = \frac{1}{(2\pi)^{3/2}} \int_0^\infty e^{-i\mathbf{k}\cdot\mathbf{r}} \psi(\mathbf{r}) d\mathbf{r},$$

where the momentum $p = \hbar k$, and $2\pi\hbar$ is Planck's quantum of action. Then the probability that the momentum lies between $\hbar k$ and $\hbar(k+dk)$ is²

$$P(k)dk = C |\phi(k)|^2 dk,$$

where C is a normalizing coefficient. This gives a measure of the fractional occupancy of the phase states; if we wish to know the number of nucleons with given momenta we must multiply by the volume of phase space available, which is proportional to $4\pi p^2 dp$. In the absence of a correct nuclear spatial wave function, it has not been possible to obtain information on momentum distributions in this manner. However, any wave functions which may be proposed in the future should be able to correctly predict the observed momentum distribution.

On the basis of a statistical gas model of the nucleus, Fermi was able to predict a momentum distribution. The nucleus is considered as a gas of neutrons and protons which is confined to a volume $\Omega = (4/3)\pi R^3$, where the nuclear radius $R = 1.5 \times 10^{-13} A^{1/3}$ cm, and A is the mass number. At ordinary nuclear excitation

energies of about 10 Mev the particles will occupy the lowest available states, for—owing to the close confinement of the particles—the energy-level spectrum has widely spaced levels. Following Fermi,³ we have for the number N of states of momentum less than p_{\max} of a proton confined to a volume Ω :

$$N = 2 \left[4\pi p_{\max}^3 \Omega / 3(2\pi\hbar)^3 \right],$$

where the factor of two takes account of the two possible orientations of a particle with spin $\frac{1}{2}$. At complete degeneracy the number of states is just equal to the number of protons, and if we assume further that $Z = A/2$ and insert the above value for Ω , we get

$$p_{\max} = (3\pi^2)^{1/3} \hbar \left(\frac{A}{2(4\pi/3)(1.5 \times 10^{-13} A^{1/3})^3} \right)^{1/3} \\ = 1.05 \times 10^{-14} \text{ cgs units,}$$

which corresponds to a kinetic energy of 21 Mev. Thus the statistical gas model predicts that all momentum states are occupied up to a maximum corresponding to about 21 Mev, and that states above this are not occupied.

For the deuteron we do have available a fairly reliable wave function, namely the Hulthén wave function $(e^{-\alpha r} - e^{-\beta r})/r$, where $(\alpha\hbar)^2 = (\text{nucleon mass}) \cdot (\text{deuteron binding energy})$ and $\beta/\alpha = 7$. This function⁴ is a close approximation to the numerical solution of the Schrödinger equation using the Yukawa potential. The value $\beta/\alpha = 7$ is obtained from the effective range theory of Blatt and Jackson.⁵ The Fourier transform of the Hulthén wave function is proportional to

$$\left| \frac{1}{\alpha^2 \hbar^2 + p^2} - \frac{1}{\beta^2 \hbar^2 + p^2} \right|^2.$$

Thus this distribution can be used as a check on the

* This work was supported by the U. S. Atomic Energy Commission.

¹ D. Bohm, *Quantum Theory* (Prentice-Hall, Inc., New York, 1951), p. 77.

² See reference 1, p. 95.

³ Fermi, Orear, Rosenfeld, and Schluter, *Nuclear Physics* (University of Chicago Press, Chicago, 1950), p. 159.

⁴ G. F. Chew, *Phys. Rev.* **74**, 815 (1948).

⁵ J. Blatt and J. D. Jackson, *Phys. Rev.* **76**, 18 (1949).

experimental procedure. Unfortunately there is no clear evidence for the validity of this distribution for high momenta.

Serber⁶ has used the Hulthén momentum distribution to explain the angular and energy distributions observed by Helmholtz *et al.*⁷ when 190-Mev deuterons are incident on various target nuclei. We consider an interaction in which the proton of the deuteron collides with a target nucleus, while the neutron does not. The neutron would continue forward with half the energy of the deuteron, except for its internal momentum with respect to the deuteron. The components of this momentum parallel to the beam direction will add to or subtract from the beam momentum of the neutron (which is half the momentum of the original deuteron) to change the energy of the emerging neutron, while the transverse components of the internal momentum will contribute to the observed angular spread of the neutrons.

The reverse of the above "stripping" process has been observed by Hadley and York,⁸ who have found deuterons and tritons produced by bombardment of various targets with 90-Mev neutrons. Since their distribution is peaked in the forward direction, and they have an energy approximately equal to that of the incident neutron, the observed deuterons could not be low energy evaporation⁹ particles. If the incident neutron finds a partner proton in the target nucleus moving with a momentum such that their relative momentum forms a state of the deuteron, then the neutron can "pick up" the proton and emerge as a deuteron. This process obviously involves the momentum distribution of the struck nucleus, as well as that of the deuteron. Chew and Goldberger¹⁰ have explained the observed distribution of deuterons, postulating a momentum distribution for carbon which fits the data. This distribution is equal to

$$\alpha/[\pi^2(\alpha^2+p^2)^2],$$

where α is a momentum corresponding to a nucleon energy of 18 Mev. Selove¹¹ has observed pick-up deuterons at various angles using 95-Mev protons. Pick-up deuterons from various target nuclei have also been observed at small angles to the beam by Bratenahl,¹² using protons of energies from 95 Mev to 138 Mev. Heidman¹³ has been able to fit York's data with an excited Fermi gas distribution with a temperature of 9 Mev. However, unless calculation and experiment are quite precise this will be indistinguishable from a gaussian distribution.

Internal momentum distributions have a profound effect on the production of mesons from nuclei; in fact,

meson production from complex nuclei tends to give more information about the structure of the nucleus than about interactions of mesons. The threshold bombarding energy can be lowered considerably, since the bombarding nucleon may encounter a target nucleon that is moving toward it with considerable momentum, which will increase the energy available in the center-of-mass system. Thus free nucleon-nucleon production of π mesons¹⁴ requires 290 Mev, while in nuclei π mesons can be produced by incident nucleons having energies as low as 180 Mev. This effect was first predicted by McMillan and Teller.¹⁵ A complete discussion of nucleonic production of π mesons in complex nuclei has been given by Henley and Huddleston¹⁶ and by Henley,¹⁷ using several momentum distributions. The distribution used affects the production threshold, excitation function, and the energy spectrum and angular distribution of the produced mesons as compared with those resulting from collisions with free nucleons used as targets. For 340-Mev protons incident, the cross section at 90° depends markedly on the nucleon momentum distribution, while at 0° the effect is not as great. This can be accounted for as follows. The produced mesons are observed¹⁸ at energies up to about 80 Mev. At 90° , the meson spectrum in free nucleon-nucleon collisions is cut off at about 9 Mev by energy-momentum conservation. Hence the form chosen for the momentum distribution, which broadens the spectrum to 80 Mev, has considerable effect. At 0° , however, the free-nucleon cutoff does not occur until about 70 Mev, so that the influence of the momentum distribution is less significant. Henley used a gaussian distribution with a $1/e$ value of 19.3 Mev, a 0°K Fermi degenerate gas model, and a modified Chew-Goldberger distribution. The Chew-Goldberger distribution mentioned above was found to have too many high-momentum components, and also has an infinite average energy. Therefore Henley suggested a modified Chew-Goldberger distribution of the form

$$[(\alpha^2+p^2)^2(\beta^2+p^2)^2]^{-1},$$

where $\beta=2.5\alpha$. This has an average energy of 48.1 Mev and still fits York's data fairly well. Nevertheless Henley found that the best fit to the experimental data was obtained from the Gaussian distribution with $1/e$ value of 19.3 Mev. Somewhat similar calculations have been performed by Block, Passman, and Havens¹⁹ for the Columbia cyclotron energy of 380 Mev; they found the best fit to be given with the original Chew-Goldberger distribution. In some later work,²⁰ however, they have used a gaussian distribution with a $1/e$ value of 14 Mev.

⁶ R. Serber, Phys. Rev. **72**, 1008 (1947).

⁷ Helmholtz, McMillan, and Sewell, Phys. Rev. **72**, 1003 (1947).

⁸ J. Hadley and H. F. York, Phys. Rev. **80**, 345 (1950).

⁹ N. Bohr, Nature **137**, 344 (1936).

¹⁰ G. F. Chew and M. L. Goldberger, Phys. Rev. **77**, 470 (1950).

¹¹ W. Selove, Phys. Rev. **92**, 1328 (1953).

¹² A. Bratenahl and B. J. Moyer, Phys. Rev. **92**, 538(A) (1953).

¹³ J. Heidman, Phys. Rev. **80**, 171 (1950).

¹⁴ R. E. Marshak, *Meson Physics* (McGraw-Hill Book Company, Inc., New York, 1952), p. 72.

¹⁵ W. McMillan and E. Teller, Phys. Rev. **72**, 1 (1947).

¹⁶ E. Henley and R. Huddleston, Phys. Rev. **82**, 754 (1951).

¹⁷ E. M. Henley, Phys. Rev. **85**, 204 (1952).

¹⁸ C. Richman and H. A. Wilcox, Phys. Rev. **78**, 496 (1950).

¹⁹ Block, Passman and Havens, Phys. Rev. **83**, 167 (1951).

²⁰ Block, Passman and Havens, Phys. Rev. **88**, 1239 (1952).

High-energy scattering experiments also provide a powerful means for studying internal momentum distributions. When 340-Mev protons are incident on a hydrogen target, the scattered protons at a given angle have a unique energy, since this is a two-body collision with the struck proton at rest. Nonrelativistically this energy is just $E_0 \cos^2\theta$, where E_0 is the incident energy and θ is the angle of observation. If the struck proton is moving inside a nucleus instead of being a free particle, the observations are somewhat different. Instead of a sharp peak, the energy spectrum is smeared out, owing to the motion of the struck proton. The faster it is moving the greater is the spread in the observed energy. Also the peak of the distribution is decreased in energy, since the binding energy of the proton knocked out and the excitation energy of the residual nucleus must be supplied by the incident proton.

Chamberlain and Segrè²¹ have bombarded lithium with 340-Mev protons, and studied the pairs of protons emitted in coincidence as a function of the angle between the two protons. Their data could be fitted by a Fermi gas momentum distribution with a maximum energy of 20 Mev. They found a peak in counting rate when the angle between their two counters corresponded to that for free nucleon-nucleon scattering. This is important evidence for the nucleon-nucleon nature of these scattering processes in light nuclei.

Cladis²² has made a more direct measurement of internal momenta. When a 340-Mev proton is incident on a nucleus, it is reasonable to think of a nucleon-nucleon collision instead of a nucleon-nucleus collision, since the De Broglie wavelength of the incident proton is comparable with the internucleon spacing in nuclei. Cladis has proposed the name "quasi-elastic scattering" for this type of event, since the process is inelastic in that a rearrangement of the nucleus is brought about, but elastic in the sense that a nucleon-nucleon collision occurs in the nucleus that resembles the scattering of nucleons by free target nucleons. Cladis observed the momentum distribution of single protons quasi-elastically scattered from carbon at 40°, and deduced the nuclear internal momentum distribution with the aid of an equation developed by Wolff,²³ which gives the energy spectrum of the nucleons scattered at a given angle as an integral over the nucleon momentum distributions. Cladis found the best fit to be a Gaussian distribution with a $1/e$ value of 16 Mev, but concluded that any Gaussian with a $1/e$ value between 14 and 19 Mev would not be inconsistent with the experimental results.

It is clear that if both protons emerging from a collision can be detected in coincidence, together with

momentum analysis of one of the protons, the event has been more explicitly defined. In this case, conservation of energy and momentum can be used, at least in the limit of the impulse approximation²⁴⁻²⁶ to definitely fix the momentum of the struck nucleon. In the present experiment the momentum distributions of protons quasi-elastically scattered from protons in various light elements have been observed under conditions that detect both particles emerging from the collision.

Chew and Wick²⁵ have given the following criteria for the validity of the impulse approximation:

(I) The incident particle never interacts strongly with two constituents of the system at the same time.

(II) The amplitude of the incident wave falling on each constituent (nucleon) is nearly the same as if that constituent were alone.

(III) The binding forces between the constituents of the system are negligible during the decisive phase of the collision, when the incident particle interacts strongly with the system.

For the case under consideration, we have:

(I) The wavelength of the incident 340-Mev proton is $\lambda = 0.22 \times 10^{-13}$ cm, while $2r_0 = 2.8 \times 10^{-13}$ cm. Thus, the wavelength of the incoming proton is smaller than the diameter of the nuclear volume for light elements, and it is reasonable to consider nucleon-nucleon collisions.

(II) The mean free path for high-energy nucleons in nuclear matter is of the order of 4×10^{-13} cm,^{27,28} which is greater than the above diameter of nuclear volume. Thus the attenuation in passing through a light nucleus should not be too great.

(III) The kinetic energies with which particles emerge from collisions in this experiment are in the region of 150 Mev, whereas the nuclear binding energy is of the order of 10 Mev, and the nuclear potential energy is of the order of 30 Mev. Thus, the energy during collision is much larger than the nuclear binding energies.

II. EXPERIMENTAL METHOD

The experiment is done with the scattered external beam of the 184-inch synchrocyclotron, which gives a 15–20 μ sec pulse of 340-Mev protons, with a repetition rate of 60 per second. The equipment is set up in the experimental area called the cave. A vertical section including the incident proton beam is shown in Fig. 1.

A. Target

The target is required to be a parallelogram by two considerations. First, the width presented to the spectrometer must be as narrow as possible in order to

²¹ O. Chamberlain and E. Segrè, *Phys. Rev.* **87**, 81 (1952).

²² J. B. Cladis, thesis, University of California Radiation Laboratory Report UCRL-1621 (unpublished), and Cladis, Hess, and Moyer, *Phys. Rev.* **87**, 425 (1952).

²³ P. A. Wolff, thesis, University of California Radiation Laboratory Report UCRL-1410 (unpublished).

²⁴ G. F. Chew, *Phys. Rev.* **80**, 196 (1950).

²⁵ G. F. Chew and G. C. Wick, *Phys. Rev.* **85**, 636 (1952).

²⁶ G. F. Chew and M. L. Goldberger, *Phys. Rev.* **87**, 778 (1952).

²⁷ A. J. Kirschbaum, thesis, University of California Radiation Laboratory Report UCRL-1967 (unpublished).

²⁸ Fernbach, Serber, and Taylor, *Phys. Rev.* **75**, 1352 (1949).

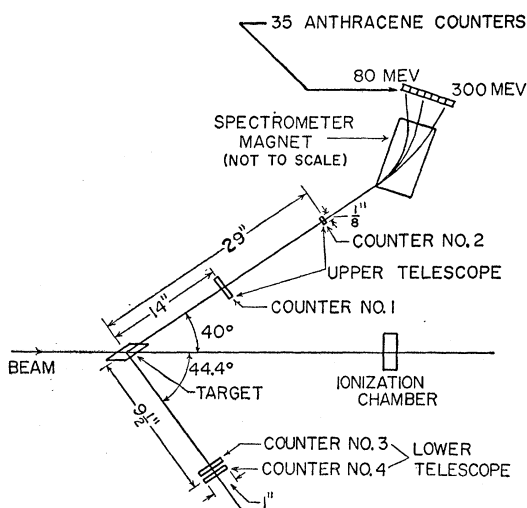


FIG. 1. Section through plane of collision.

preserve good energy resolution, and second, the length of target through which the protons must pass after a scattering event must be as small as possible in order to reduce energy losses in the target. Hydrogen and deuterium were observed in the form of CH_2 and CD_2 , with an appropriate subtraction being made for the effect of the carbon. A very thin coating of aluminum was evaporated in a vacuum on the lithium target to protect it from contamination in the air. The boron target was sintered into the proper shape. A one-mil aluminum foil was needed to hold it together.

B. Counter Telescopes

The two protons emerging from a collision are detected in coincidence by two counter telescopes, consisting of *trans*-stilbene crystals viewed by 1P21 photomultiplier tubes. It is desirable that protons pass through the upper telescope without deviation, so that they will enter the energy spectrometer in the proper direction. Therefore, the thickness of these crystals that the protons pass through was one-eighth of an inch. Counter No. 2 defines the path of particles into the spectrometer; therefore, its width (measured in the plane of collision) must be made as narrow as possible, consistent with an adequate counting rate. Counters No. 3 and No. 4 are made thicker, since small-angle scattering does not matter. Counter No. 4 defines the path of particles detected by the lower telescope. It is a rectangle one inch long in the plane of collision and two inches long perpendicular to this plane.

Since crystal counters No. 1 and No. 2 are made very thin to avoid multiple scattering, the protons lose a small amount of energy in passing through, and thus an efficient light-collecting system must be employed. Each crystal is viewed from both ends by 1P21 photomultiplier tubes, with an aluminum housing of the size of the photocathodes to permit maximum light collection.

C. Energy Spectrometer

1. Description.—The momentum of the upper proton is measured with a bending magnet and a row of 35 anthracene counters, viewed by 931A or 1P21 photomultiplier tubes. The scattered beam emerges into the cave in the form of a line approximately one-sixteenth inch wide, which is tilted at 13 degrees from the horizontal, as shown in Fig. 2. It was desired to have this line serve as a line source for the spectrometer, i.e., the pole faces of the magnet should be perpendicular to it. Thus it was necessary to build a steel stand to hold the seven-ton magnet six feet above the floor, tilted at an angle of 13 degrees. The target holder was fastened to this stand, and the base for the 35 anthracene crystals was also permanently attached, making it possible to do all aligning and calibrations outside the cave. For a run the whole assembly was lifted into the cave with the overhead crane.

2. Resolving Power of Particle Spectrometer.—The resolving power of the spectrometer depends on (1) the target width considered as a slit, (2) the width of telescope counter No. 2, (3) the widths of the 35 anthracene crystals, (4) the energy loss of protons in the targets, and (5) the small-angle scattering in telescope counter No. 2. The over-all resolving power of the spectrometer is obtained by "folding" together the widths due to each of the above factors. This process has been described in detail in a previous report.²² The spectrometer resolution can be checked experimentally at the energy corresponding to scattering from a hydrogen target. Such protons are monoenergetic, and the shape and width of the observed spectrum represents the resolution of the equipment. This was approximately 20 Mev (full width at half-height) for this experiment (see Fig. 4).

3. Nature of Scattered Particles Detected.—Mesons

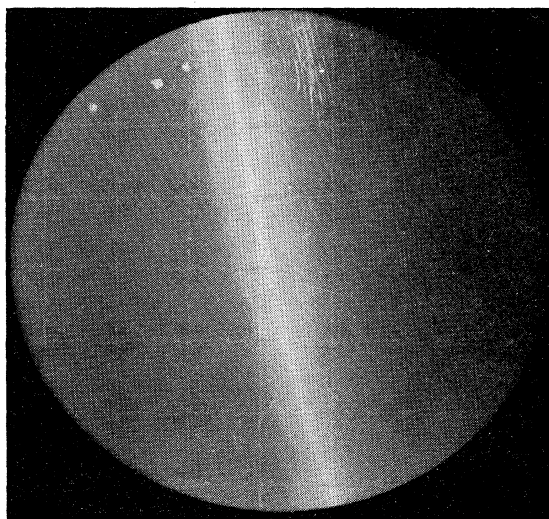


FIG. 2. Scattered proton beam.

will not reach even the lowest energy channel unless they have an energy greater than 300 Mev. The number of deuterons and alpha particles entering the spectrometer had been measured (without demanding correlated particles) by Hess with an absorber technique²⁹ and found to be less than five percent. When a correlated particle technique is used the deuteron and alpha-particle contamination is greatly reduced below this figure, since the angular correlation demanded by this experiment greatly favors protons. It is therefore assumed that all particles with which we are here involved are protons.

D. Electronics

A block diagram of the electronics is shown in Fig. 3. Signals from the 1P21 photomultipliers that view the crystals in the telescopes go through an adder-and-shaping circuit to a coincidence circuit³⁰ which, with these shaped pulses, operates with a resolving time of 5×10^{-9} sec. Signals from the 35 counters in the spectrometer are amplified and trip a one-shot multivibrator which in turn actuates a mechanical counter. The output of the coincidence circuit is counted on a scaler, and also makes a $0.4 \mu\text{sec}$ gate which turns on the 35-channel amplifiers.

E. Monitor

An argon-filled ionization chamber was used to monitor the beam current to which the target was exposed. The scattering of the beam by the various targets introduces a negligible error in the monitor readings.

III. EXPERIMENTAL PROCEDURE

The exact height of the line distribution of the scattered proton beam is first determined with a photographic film. Since this height drifts slightly from time to time, owing to unknown causes, it is necessary to shoot a film every few hours during the run. With the beam at a fixed level, plateaus are obtained of telescope coincidences per monitor as a function of photomultiplier voltage and of linear amplifier gain. The time at which the coincidence gate is sent out to the 35-channel amplifiers is then varied to achieve the optimum counting rate.

Two types of accidentals may occur: (1) in the telescope quadruple coincidence circuit, (2) between a 35-channel counter and the telescope gate. Both types can be measured by changing the beam level. The second type can also be measured by inserting a $2 \mu\text{sec}$ delay in the telescope gates sent out to the 35-channel amplifiers, so that the gate could not coincide with a real pulse. Results of these two methods are in agreement.

²⁹ W. N. Hess (private communication).

³⁰ R. Madey and K. Bandtel, Rev. Sci. Instr. (to be published); University of California Radiation Laboratory Report UCRL-1880 (unpublished).

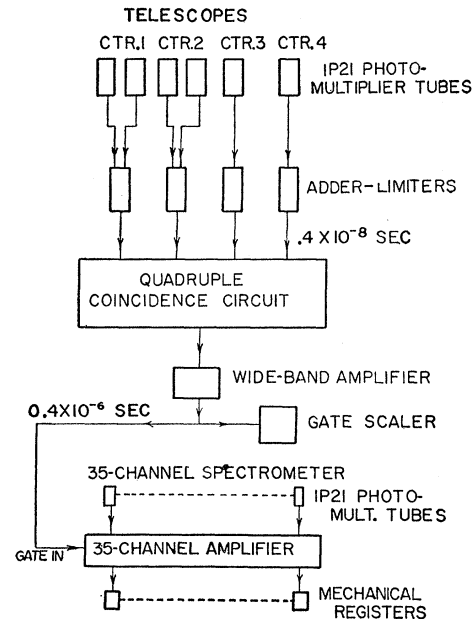


FIG. 3. Block diagram of electronics.

The following data are recorded for each run: (1) number of gates, (2) the integrated beam, (3) the time interval, and (4) the readings of the 35 registers. Repeated runs on various targets are made in sequence to minimize the effects of long-term drifts. The beam intensity is kept constant so that there is a constant proportion of accidentals for a given target.

IV. ANALYSIS OF DATA

A. Subtraction of Accidentals

The spectrum obtained from the 35 registers must be corrected for the two types of accidental counts mentioned above. The greatest number of counts resulting from telescope accidentals may be expected when one proton passes through the top telescope and another particle, which is not a companion proton from the same collision, passes through the bottom telescope. Thus the channel counts arising from this type of accidental gate should have a spectrum similar to that obtained by gating the 35 amplifiers by the upper telescope only. This accidental spectrum is subtracted out. The remaining spectrum is made by true correlated proton gates, but there are still accidentals between the 35 channel pulses and the gates. This accidental spectrum is determined by delaying the gates by $2 \mu\text{sec}$ as described in the aforementioned, and subtracted out.

B. Channel Efficiencies

Each of the 35 channel counters has a different energy width for accepting protons, ranging from 15 Mev at the high-energy end to 2.2 Mev at the low end. Thus, the counts in each channel must be divided by its energy width to give a true number of counts per

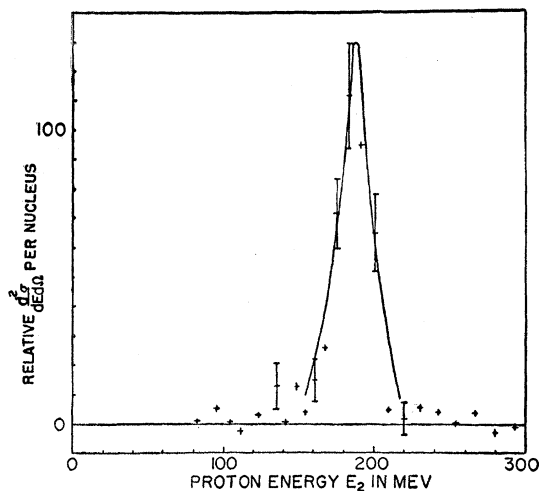


FIG. 4. Proton energy spectrum from hydrogen.

unit energy interval. Several channels at the low energy end are added together to make the energy widths at all parts of the spectrometer more nearly uniform.

The spectrum thus obtained includes the effects of the finite size of the telescope counters and the spectrometer resolution. These effects must be folded into a theoretical momentum distribution before it can be compared with the data.

C. Kinematics of Process

The relation between a value of the target proton momentum and the momentum of an observed proton was calculated from relativistic conservation of energy and momentum. (See Appendix.) The binding energy of the nuclear proton and an estimated excitation energy of 10 Mev for the residual nucleus were added into the conservation-of-energy equation. It must be observed that this experiment compels the struck nucleon to be moving in a well-defined direction. Consider the upper telescope to be a point counter, with the bottom telescope subtending a finite solid angle Ω_3 . Then for nuclear protons of energy E_5 , only those moving within a fixed solid angle Ω_5 can be counted. Furthermore, the size of Ω_5 depends on the energy E_5 of the nuclear proton. When its energy approaches zero, it is similar to a proton at rest, and every proton in the upper telescope resulting from a collision has its partner detected in the lower telescope. If, on the other hand, the energy E_5 of the nuclear proton is very large, only those protons which were moving within a small cone of solid angle Ω_5 are counted. The value of Ω_5 corresponding to each value of E_5 was computed numerically, as explained in the Appendix. Thus, an assumed momentum distribution must first be multiplied by this solid-angle efficiency factor. The distribution is then corrected for the finite widths of the telescope counters. (See Appendix.) Finally, the resolution of the spectrometer is folded in. The resulting

spectrum can then be compared with the experimental data.

The point involved in the discussion of the solid angle Ω_5 may be clearer if we consider a simple analogy. Consider the collision of two nonrelativistic particles of equal mass which are to be detected after the collision by point counters 90° apart. There is a definite restriction on the angle with which the struck particle was moving before the collision, since conservation of energy and momentum will require that before the collision the struck particle had to be moving perpendicularly to the incident particle. This same general type of effect carries over into the more complex problem considered in this experiment.

V. RESULTS

A. Hydrogen

The spectrum obtained from hydrogen is shown in Fig. 4. This is an experimental check of the resolution of the spectrometer, since protons scattered from hydrogen at a fixed angle are monoenergetic. The full width at half height is about 20 Mev, which agrees with the value calculated from the above spectrometer resolution theory. The solid curve is only to guide the eye but is consistent with the resolution curve generated out of the parameter widths mentioned in Sec. II-C-2. The errors shown in all curves are standard deviations.

B. Deuterium

The spectrum obtained from deuterium is shown in Fig. 5. This isotope was observed in order to check the experimental method used, since its momentum distribution is fairly well known.³¹ The solid curve was

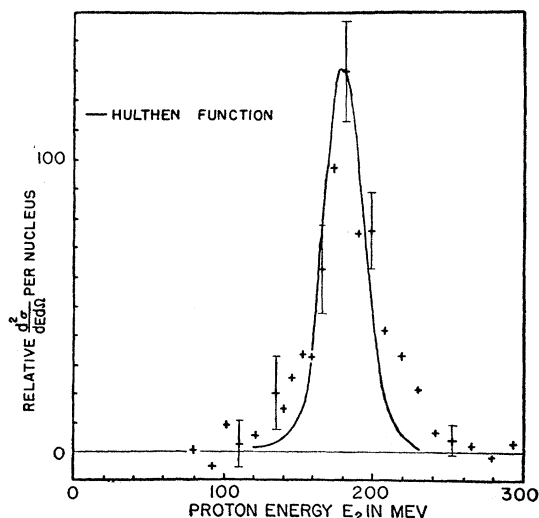


FIG. 5. Proton energy spectrum from deuterium.

³¹ This is given by the square of the Fourier transform of the Hulthén wave function $(e^{-\alpha r} - e^{-\beta r})/r$, where $\beta = 7\alpha$ and $(\alpha\hbar)^2 = (\text{nucleon mass}) \cdot (\text{deuteron binding energy})$. This distribution is proportional to

$$\left[\frac{1}{\alpha^2 \hbar^2 + p^2} - \frac{1}{\beta^2 \hbar^2 + p^2} \right]^2.$$

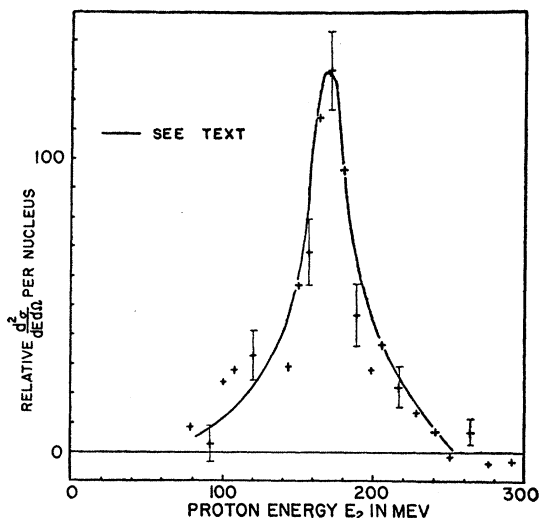


FIG. 6. Proton energy spectrum from lithium.

computed from this distribution by the method outlined previously. Since this curve lies inside the experimental points at its edges, the simple wave function used here does not lead to enough high-momentum components. However, the experimental errors due to subtraction of the carbon spectrum and accidentals are large in this region, since the experiment was not designed to view a narrow distribution such as that from the deuteron.

C. Lithium

The spectrum obtained from lithium is shown in Fig. 6. The shape is rather similar to that obtained from the deuteron. The narrow peak in the center may be due to the unpaired protons having lower kinetic energy than the two paired protons. The peak occurs at an energy 12 Mev lower than the hydrogen peak. The binding energy of the proton knocked out of the lithium (10 Mev) and the excitation energy given to the recoil nucleus (estimated to be 10 Mev) must be given up by the two recoiling protons. Thus we could expect the peak to be shifted by approximately the observed amount. The solid curve is explained in Sec. VI-B.

D. Beryllium

The spectrum obtained from beryllium is shown in Figs. 7 and 8. The best fit is obtained from a Gaussian momentum distribution with a $1/e$ value of about 20 Mev, although—as shown in Fig. 7—Gaussians with $1/e$ values of 16 and 25 Mev can fit the data. The Gaussian distributions are too low at the high-energy tail, but this is the region where the impulse approximation is less valid, and also the errors from subtraction of the background become large. Curves obtained from a degenerate Fermi gas distribution (square distribution) are shown in Fig. 8, with Fermi energies of 15 and 25 Mev. These do not fit as well as the Gaussian. Figure 8 also

shows a Chew-Goldberger¹⁰ distribution,³² which appears to be too narrow.

E. Boron

The spectrum obtained from boron is shown in Fig. 9. The solid curve is to guide the eye to the boron points, while the dashed curve is a best fit to the beryllium points, for comparison. The distribution is more peaked than that of beryllium; this may be owing to the presence of an unpaired proton which is moving with lower kinetic energy.

F. Relative Yield

The relative yield per nuclear proton was as follows:

	Observed	Calculated
Hydrogen	100	100 (assigned)
Deuteron	36	33.6
Lithium	13.3	
Beryllium	4.4	6.5
Boron	5.1	

In order to obtain an adequate counting rate with good spectrometer energy resolution, it was necessary to use targets of varying dimensions. The spatial distribution of the proton beam varies considerably (Fig. 2). Therefore the above observed yields can be considered to indicate only the general trends involved.

The observed relative yield provides a good check on the internal consistency of the experiment. As explained previously, each value of the struck-proton

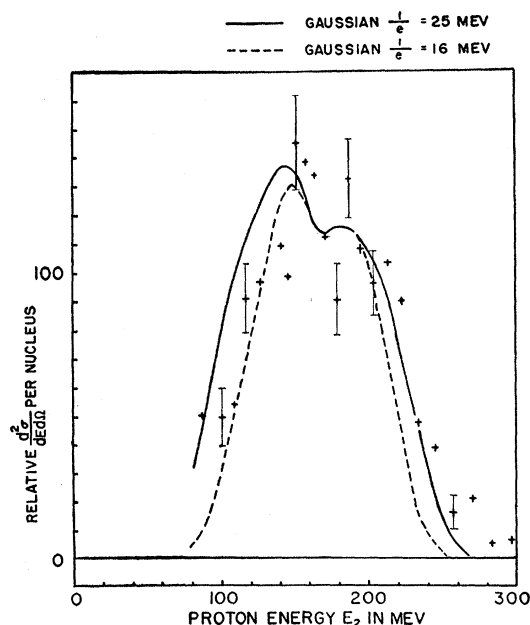


FIG. 7. Proton energy spectrum from beryllium (Gaussian).

³² The Chew-Goldberger momentum density distribution is

$$N(p) = (\text{const}) \cdot a / (a^2 + p^2)^2,$$

where p is the nucleon momentum and a is a momentum corresponding to a nucleon energy of 18 Mev.

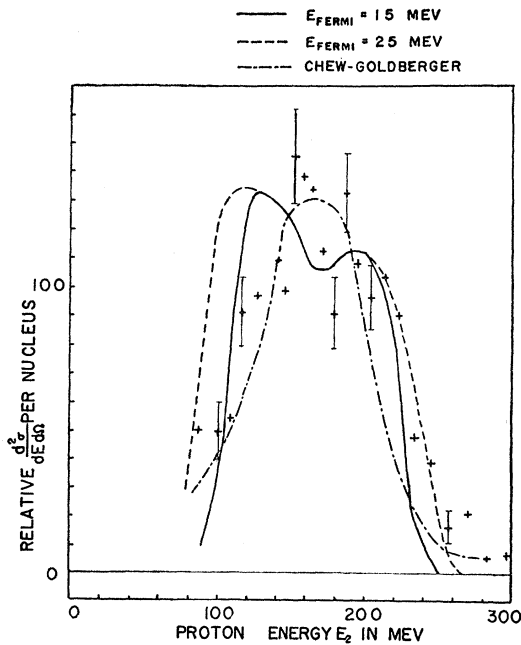


FIG. 8. Proton energy spectrum from beryllium (E_{Fermi}).

momentum has associated with it a definite solid angle Ω_5 within which the struck proton must have been moving before the collision, in order that the correlated protons emerging from the collision can be seen by the counters. These solid angles have been computed for deuterium and beryllium. If we now calculate an average solid angle for each element, then the ratios of these average solid angles should be just equal to the ratios of the observed yield. For hydrogen, the appropriate solid angle is 4π , since the struck proton is at rest and hence has no directional limitations imposed on it. For the complex nuclei, the average solid angle is computed as

$$\bar{\Omega}_5 = \int_0^\infty [\Omega_5(E_5)] N(E_5) \sqrt{E_5} dE_5 / \int_0^\infty N(E_5) \sqrt{E_5} dE_5;$$

i.e., each value of the solid angle $\Omega_5(E_5)$ is weighted by the number of nuclear protons that have an energy of E_5 . In the above formula $N(E_5)$ is the density of states of energy E_5 , and $(\sqrt{E})dE$ is proportional to $p^2 dp$, which is proportional to the volume of phase space available to a particle of momentum p . For the deuteron $N(E_5)$ was obtained from the Hulthén wave function, and for beryllium $N(E_5)$ was obtained from a Gaussian momentum density distribution with a $1/e$ value of 16 Mev. This check turned out quite well, as can be seen in the above table. When comparing the observed and calculated yields for beryllium, one should remember that there is a certain fraction of double collisions in beryllium—that is, where one of the correlated protons emerging from a collision suffers a further nucleon-nucleon collision in the same nucleus. These

events are not counted, since in general the angular correlation of the protons is lost. Wolff²³ has calculated that one-half of the collisions of 340-Mev protons on carbon will be of this type. If one assumes a loss of one-third for beryllium, and reduces the calculated yield by this amount, a good agreement is obtained with the observed yield.

VI. CONCLUSIONS

A. Quantitative Results from Beryllium

This experiment has indicated that the beryllium momentum-density distribution is best approximated by a Gaussian function with a $1/e$ value of 15 to 25 Mev, with the best value of about 20 Mev. This is in good agreement with the results for carbon of Henley¹⁷ and Cladis.²² In examining nucleonic production of π mesons in complex nuclei, Henley found the best fit with a Gaussian momentum distribution with a $1/e$ value of 19.3 Mev. With the nucleon scattering experiment previously described, Cladis found the best fit to be a Gaussian distribution with a $1/e$ value of 16 Mev. The Chew-Goldberger¹⁰ distribution, which was used by these authors to explain the production of deuterons by the pickup process, gave a poorer fit in this experiment the Gaussian. The completely degenerate Fermi distribution (rectangular curve) gave the poorest fit of all. An excited Fermi distribution, however, will resemble a Gaussian within the accuracy of this experiment.

As pointed out in Sec. IV-C, the experimental efficiency for observing nuclear protons having a large momentum is much less than the efficiency for ob-

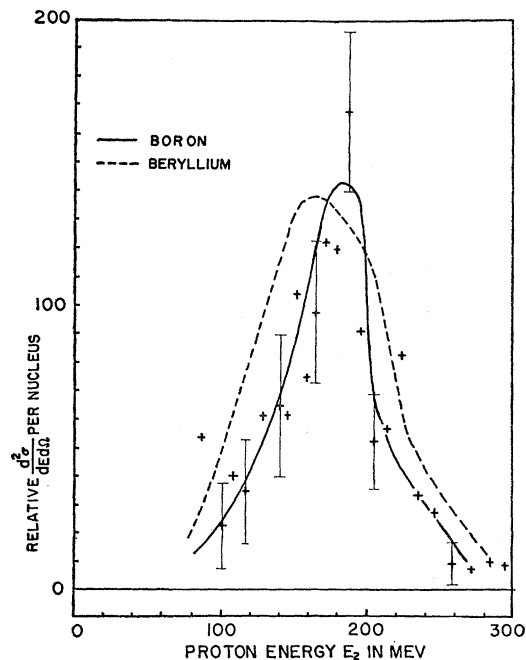


FIG. 9. Proton energy spectrum from boron.

serving nuclear protons having a small momentum. Thus very high momentum values contribute very little, and the results are not statistically significant. The results given here do not disagree with the paper of Selove,¹¹ who finds from studying a pickup process that there is a very high energy tail to the internal momentum distributions.

B. Qualitative Results from H, D, Li, Be, and B

The narrow peak of the experimental spectrum obtained from hydrogen establishes the spectrometer resolution. The observed curve from the deuteron is only slightly wider, as would be expected, because the binding energy is only 2.2 Mev. It is well known that the deuteron spends more than half the time outside the potential well. In the exterior region (which is classically forbidden), the wave function has the form $\psi = Ae^{-\alpha r}/r$, where $\alpha = (2MB/\hbar^2)^{-1/2}$, M = nucleon mass, B = binding energy, and A is a constant. The expectation value of the kinetic energy in the exterior region then is B .

Owing to the difficulties in working with a helium target, no spectrum was obtained from helium; however, since the alpha particle is a tightly bound, stable structure, one might expect a considerable average kinetic energy.

The lithium spectrum consists of a broad base with a peak at the center which is very similar to the peak observed from the deuteron. In lithium we could postulate two types of protons: two protons with considerable average kinetic energy which belong to the "core" of the nucleus, and a third proton which has considerably less momentum, comparable, in fact, to that of the proton in the deuteron. This hypothesis has been compared with the experimental data in two ways, first by comparing the relative yields from the deuteron, lithium, and beryllium, and secondly by predicting the shape of the observed lithium spectrum by using the spectra from the deuteron and beryllium.

The reason that the relative-yield data are significant is that the efficiency of detection of collisions depends on the energy of the struck proton, as has been explained previously. Thus the slowly moving proton in the deuteron has a large probability of being counted, because of the large solid angle Ω_5 associated with it, as explained in IV-C, while the more energetic protons in beryllium are counted with a lower efficiency. If we assume that the two "core" protons in lithium are moving similarly to the protons in beryllium, and thus are counted at the beryllium rate, and that the third proton is being counted at the deuteron rate, we can predict a yield (per nuclear proton) from lithium on the basis of the yield of 36 from the deuteron and 4.4 from beryllium. The calculated lithium yield of 14.9 is consistent with the observed yield of 13.3.

The shape of the lithium spectrum can now be predicted from the shapes of the deuteron and beryllium spectra. If we normalize all these spectra on the basis

of the observed yields (i.e., the area under the curve is proportional to the yield), and then add twice the beryllium spectrum (representing the two lithium "core" protons) to the deuteron spectrum (representing the single lithium proton outside the core) we get the predicted spectrum for lithium. The curve obtained in this manner is the solid line drawn in Fig. 6, and is seen to be in good agreement with most of the experimental points.

All the current nuclear models, including Maria Mayer's very successful shell model,³³ put the third proton in lithium in a p state of orbital angular momentum, since the two lowest-energy S states available (spin up and spin down) have already been occupied by the two "core" protons. The binding energy of the last proton in Li⁷ is 10.1 Mev, but its average kinetic energy is just a few Mev; therefore this proton would not be like that in the deuteron and would not be expected to spend much time in the region exterior to the potential well.

The spectrum obtained from beryllium was considerably broader than that from lithium. As explained above, the beryllium spectrum has been fitted by assuming a Gaussian momentum-density distribution for all the protons in beryllium with a $1/e$ value of about 20 Mev. To the extent that the alpha-particle model is valid, and that Be⁹ is composed of two alpha subgroups plus an extra neutron, it is reasonable to assume that all the protons in beryllium have similar momentum distributions.

The spectrum observed from boron was in general similar to that from beryllium, except that it is somewhat narrower. This could be explained on grounds that the fifth proton in boron is somewhat like the third proton in lithium discussed above. Since this proton is one of five, the percentage effect would be smaller.

Because the binding energy for the "last" proton in Li⁶ is distinctly different from that in Li⁷ it would be very desirable to employ separated isotopes in this investigation; and a similar remark can apply to B¹⁰ and B¹¹. The smallness of available targets of isotopic purity in elemental form makes it unreasonable to pursue this refinement under the present techniques.

ACKNOWLEDGMENTS

Wilmot Hess worked with the experiment in the early stages, and George Merkel has helped in the final runs and interpretation of the data. Many valuable theoretical discussions were held with Warren Heckrotte, Robert Karplus, and Malvin Ruderman. Wilson Frank and Kenneth Bandtel gave invaluable assistance with the fast-coincidence gear. Finally, thanks are due James Vale, Lloyd Houser, and the members of the cyclotron crew.

³³ M. G. Mayer, Phys. Rev. **78**, 16 (1950).

APPENDIX

Kinematics (See Fig. 10)

The analysis begins with the four relativistic equations which express conservation of energy and momentum:

Conservation of energy:

$$\gamma_1 m + M = \gamma_2 m + \gamma_3 m + \gamma_4 M' \quad (1)$$

Conservation of Z momentum (incident particle enters along Z axis):

$$m\alpha_1 = m\alpha_2 \cos\theta_2 + m\alpha_3 \cos\theta_3 + M'\alpha_4 \cos\theta_4 \quad (2)$$

Conservation of X momentum:

$$0 = m\alpha_2 \sin\theta_2 \cos\phi_2 + m\alpha_3 \sin\theta_3 \cos\phi_3 + M'\alpha_4 \sin\theta_4 \cos\phi_4 \quad (3)$$

Conservation of Y momentum:

$$0 = m\alpha_2 \sin\theta_2 \sin\phi_2 + m\alpha_3 \sin\theta_3 \sin\phi_3 + M'\alpha_4 \sin\theta_4 \sin\phi_4 \quad (4)$$

where m = mass of proton, M = mass of struck nucleus, M' = mass of recoiling nucleus + ϵ/c^2 , ϵ = excitation energy of recoiling nucleus, $\gamma = 1 + (\text{kinetic energy})/(\text{rest mass energy})$, and $\alpha = (\gamma^2 - 1)^{1/2}$. Note that $m\alpha$ represents momentum.

We can first show that the momentum of the struck nucleon is completely determined by the quantities measured experimentally. Before the collision occurs all parameters are known, since the nucleus is at rest and the direction and energy of the incident beam proton are known. After the collision the energy and direction of proton number 2 and the direction of proton number 3 are measured. Thus there remain four

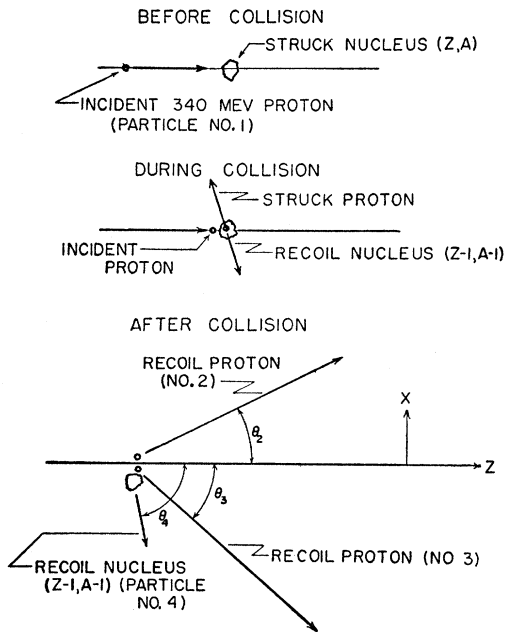


FIG. 10. Kinematics of collision.

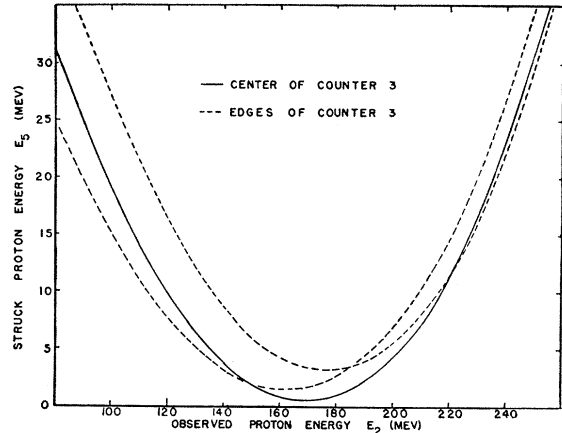


FIG. 11. E_5 vs E_2 for beryllium.

unknown quantities: the energy of proton number 3 and the energy and direction (two angular variables) of the recoil nucleus. The four equations involving conservation of energy and momentum are then sufficient to completely define the collision.

Since the nucleus was originally at rest, the struck nucleon must have been moving with momentum equal and opposite to that of the recoiling nucleus. The energy of a proton having the same momentum as the recoiling nucleus is designated E_5 .

The solid angle Ω_5 in which the struck nucleon must be moving is calculated numerically. The equations of motion are first solved for the emerging protons passing through the centers of the telescope counters, and then for the emerging protons passing through the corners of telescope counter No. 3. Telescope counter No. 2 is assumed to be a point counter, since its dimensions are an order of magnitude smaller than counter No. 3. Thus the extreme directions of struck nucleon momentum are determined, and the solid angle Ω_5 is defined. The calculations are repeated for a range of values of struck proton momentum, and Ω_5 is determined as a function of E_5 .

The proton-proton differential scattering cross section is approximately independent of energy and angle in the c.m. system at these energies. However, since the struck proton is moving, the transformation of solid angle from the c.m. system to the laboratory system will change slightly from event to event. This change has been calculated numerically and found to amount to less than 5 percent.

In general a particle with momentum p has available phase space proportional to $p^2 dp$, or $(\sqrt{E})dE$, since $p^2 = 2ME$. However, for this problem the available phase space is only a fraction of the total, namely $(\Omega_5/4\pi)(\sqrt{E_5})dE_5$. Thus the number of detectable collisions produced by nuclear protons moving with an energy between E_5 and $E_5 + dE_5$ will be proportional to $N(E_5)(\Omega_5/4\pi)(\sqrt{E_5})dE_5$, where $N(E_5)$ is the energy distribution of the nuclear protons. These collisions

will result in scattered protons in telescope counter number 2 having a small range in values of E_2 . Thus each value of E_5 results in a distribution of protons about a particular value of E_2 . The observed spectrum $N(E_2)$ can be obtained by graphical addition of the contributions from all values of E_5 .

Figure 11 shows the relationship between the struck proton energy E_5 and the observed proton energy E_2 for beryllium. The solid curve is for the case of a proton going through the center of telescope counter number 3, while the dashed curves represent protons which go through the sides of telescope counter number 3. Thus this figure indicates the effects of the finite size of this counter. It should be noted that a given value of E_2 on the left-hand half of the curve ($E_2 < 170$ Mev) corresponds to a rather wide range in values of E_5 , whereas a given value of E_2 on the right-hand half of the curve

($E_2 > 170$ Mev) corresponds to a smaller range in values of E_5 . Thus for a flat-topped momentum distribution such as the Fermi (rectangular), contributions from many values of E_5 will add up at a particular value of E_2 to produce the characteristic double-peaked curves. However, in the somewhat narrower Chew-Goldberger distribution this effect is largely washed out.

It should be further noted that each value of E_5 corresponds to two values of E_2 . Thus the information comes in twice, i.e., either the left half or the right half of the experimental curves would determine the nuclear momentum distribution. The agreement of the experimental points with both halves of the calculated curves thus gives a measure of the internal consistency of the experiment.

The nuclear momentum distribution is assumed to be isotropic.

Diffusion Cloud-Chamber Study of Very Slow Mesons.* II. Beta Decay of the Muon

C. P. SARGENT,† M. RINEHART, L. M. LEDERMAN, AND K. C. ROGERS
Department of Physics, Columbia University, New York, New York

(Received April 8, 1955)

The spectrum of electrons arising from the decay of the negative mu meson has been determined. The muons are arrested in the gas of a high-pressure hydrogen-filled diffusion cloud chamber. The momenta of the decay electrons are determined from their curvature in a magnetic field of 7750 gauss. The spectrum of 415 electrons has been analyzed according to the theory of Michel. The shape parameter, ρ , is found to be 0.64 ± 0.10 . The significance of this result in terms of the beta interaction is discussed.

A. INTRODUCTION

THE determination of the spectrum of electrons which are produced by the decay of the muon is one of the most honored problems in particle physics.¹⁻¹⁰ Some of the difficulties in arriving at definite conclusions from the mass of data are discussed by Williams.⁹ One of the principal difficulties is the generally poor resolution that has been used. The earlier data were not accompanied by detailed discussions of the resolution of the respective techniques. The lack of resolution was principally due to radiation losses of the decay electrons in the material used to arrest the muons.

The present experiment employs the gas of a hydrogen-filled diffusion cloud chamber working at a pressure

of 19 atmospheres, to stop negative muons and to observe the momentum of the decay electrons. The experimental arrangement has already been reported.¹¹ In addition to the negligible radiation and ionization losses, the lack of dead mass allows an examination of the entire spectrum. This virtue eliminates the necessity of arbitrarily normalizing the data.

B. EXPERIMENTAL CONSIDERATIONS

Negative mesons from the 60-Mev pion beam of the Nevis cyclotron are moderated and allowed to enter the diffusion chamber, where a small fraction of pions and muons spiral to rest in the gas (see Fig. 1). Muon endings are scanned for associated decay-electrons. Momenta of the electrons are determined from curvature and angle measurements and from the value of the magnet field ($\bar{H} = 7750$ gauss) at the time of the event.

Because of the finite depth of the sensitive layer, the visible path length of roughly half of the decay electrons is so short that their inclusion in the data would seriously impair momentum resolution. The mesons decay from Bohr orbits, and hence any criterion which requires that the electrons be emitted within some

* This research was supported in part by the joint program of the Office of Naval Research and the U. S. Atomic Energy Commission.

† Now at Laboratory for Nuclear Science, Massachusetts Institute of Technology, Cambridge, Massachusetts.

¹ R. Thompson, Phys. Rev. **74**, 490 (1948).

² J. Steinberger, Phys. Rev. **75**, 1136 (1948).

³ Leighton, Anderson, and Seriff, Phys. Rev. **75**, 1432 (1949).

⁴ A. Lagarrigue and C. Reyrou, Compt. rend. **233**, 478 (1951).

⁵ Davies, Lock, and Muirhead, Phil. Mag. **40**, 1250 (1949).

⁶ Sagane, Gardner, and Hubbard, Phys. Rev. **82**, 557 (1951).

⁷ H. Bramson and W. Havens, Phys. Rev. **88**, 304 (1952).

⁸ R. Levisetti and G. Tomasini, Nuovo cimento **8**, 12 (1951).

⁹ J. Vilain and R. Williams, Phys. Rev. **94**, 1011 (1954).

¹⁰ Sagane, Dudziak, and Vedder, Phys. Rev. **95**, 863 (1954).

¹¹ Sargent, Cornelius, Rinehart, Lederman, and Rogers, Phys. Rev. **98**, 1349 (1955); referred to as I.

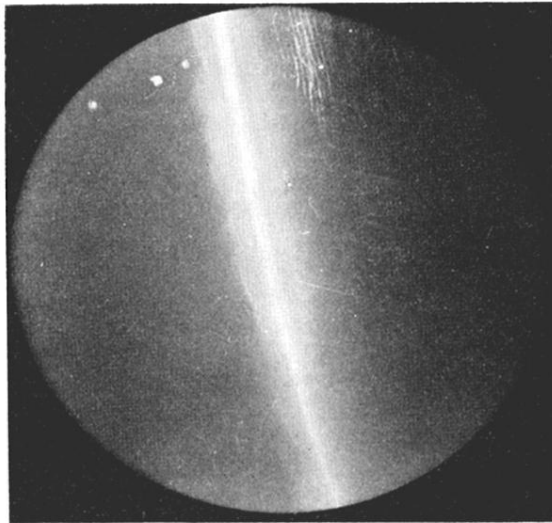


FIG. 2. Scattered proton beam.